

Received: 30 July 2010,

Revised: 12 October 2010,

Accepted: 12 October 2010,

Published online in Wiley Online Library: 2011

(wileyonlinelibrary.com) DOI:10.1002/jmr.1109

Single and multiple bonds in (strept)avidin–biotin interactions[†]

Jean-Marie Teulon^a, Yannick Delcuze^a, Michael Odorico^a,
 Shu-wen W. Chen^a, Pierre Parot^a and Jean-Luc Pellequer^{a*}

Thanks to Dynamic Force Spectroscopy (DFS) and developments of massive data analysis tools, such as YieldFinder, Atomic Force Microscopy (AFM) becomes a powerful method for analyzing long lifetime ligand–receptor interactions. We have chosen the well-known system, (strept)avidin–biotin complex, as an experimental model due to the lack of consensus on interpretations of the rupture force spectrum (Walton *et al.*, 2008). We present new measurements of force–displacement curves for the (strept)avidin–biotin complex. These data were analyzed using the YieldFinder software based on the Bell-Evans formalism. In addition, the Williams model was adopted to interpret the bonding state of the system. Our results indicate the presence of at least two energy barriers in two loading rate regimes. Combining with structural analysis, the energy barriers can be interpreted in a novel physico-chemical context as one inner barrier for H-bond ruptures ($\gamma < 1 \text{ \AA}$), and one outer barrier for escaping from the binding pocket which is blocked by the side chain of a symmetry-related Trp120 in the streptavidin tetramer. In each loading rate regime, the presence of multiple parallel bonds was implied by the Williams model. Interestingly, we found that in literature different terms created for addressing the apparent discrepancies in the results of avidin–biotin interactions can be reconciled by taking into account multiple parallel bonds.

Copyright © 2011 John Wiley & Sons, Ltd.

Keywords: avidin; streptavidin; biotin; single bond; multiple bond; interaction; lifetime; atomic force microscopy (AFM)

INTRODUCTION

Short history of avidin–biotin interactions

Avidin

Avidin was discovered by Snell and coworkers (Eakin *et al.*, 1940). The road to discovery has been described in details by Kresge (2004). It began with the observation on chicks that became deficient in biotin (vitamin B₇ or vitamin H) on a diet of raw egg-white, even though biotin was available in their diet. It was thought that a component in the egg-white was sequestering biotin. Therefore, the protein was tentatively named avidalalbumin, yet later it has been revised to avidin due to its high affinity for biotin.

Avidin accumulates in albumen (egg-white) and is produced in the oviducts of birds, reptiles, and amphibians. In chicken egg white, avidin makes up approximately 0.05% of total proteins (about 1.8 mg per egg). Avidin is glycosylated (10% of the molecular weight) and positively charged; it has a pseudo-catalytic activity (i.e., enhancing alkaline hydrolysis of the ester chemical bond between biotin and a nitrophenyl group), and exhibits a high tendency toward aggregation. Avidin is a tetrameric protein (66–69 kDa in size (Korpela, 1984)) with four identical subunits, each of which can bind to biotin with high affinity and specificity. The apparent dissociation constant (K_d) of avidin is about 10^{-15} M , one of the strongest non-covalent interaction known (Green, 1963a; Green, 1963b; Green, 1963c; Melamed and Green, 1963).

Streptavidin

Streptavidin is a protein evolutionarily unrelated to avidin, and it can be purified from the bacterium *Streptomyces avidinii*. Although the biological function of streptavidin remains

unknown, this molecule shows very similar properties to that of avidin. Streptavidin is a tetrameric protein of 52.8 kDa, it has been widely used in molecular biology because of its extraordinarily strong affinity for biotin (Wilchek and Bayer, 1990), standing together with avidin–biotin as the strongest non-covalent interactions in nature.

The secondary, tertiary, and quaternary structures of streptavidin are almost identical to those of avidin despite the fact that they share only 30% of sequence identity. Compared to avidin, streptavidin has a slightly lower affinity for biotin ($K_d \sim 10^{-14} \text{ M}$) with a mildly acidic isoelectric point (pl) of ~5. Taken together with the near-neutral pl and lacking of carbohydrate modification, streptavidin exerts much lower non-specific binding than avidin to biotin. Nevertheless, deglycosylated avidin (NeutrAvidin) has comparable size, pl, and non-specific binding strength as streptavidin does.

Biotin

On account of Green's description (1975), avidin is only part of the great story of discovery, isolation, and synthesis of biotin. Biotin was identified in 1935 by Koegl and Tönnis (1936), it is a

* Correspondence to: Jean-Luc Pellequer, CEA Marcoule, DSV/IBEB/SBTN, Bat 170, BP 17171, 30207 Bagnols sur Cèze, France.
 E-mail: jl.pellequer@cea.fr

a J.-M. Teulon, Y. Delcuze, M. Odorico, S.-w. W. Chen, P. Parot, J.-L. Pellequer CEA, IBEB, Service de Biochimie et Toxicologie Nucléaire, F-30207 Bagnols sur Cèze, France

† This article is published in Journal of Molecular Recognition as a focus on AFM on Life Sciences and Medicine, edited by Jean-Luc Pellequer and Pierre Parot (CEA Marcoule, Life Science Division, Bagnols sur Cèze, France).

water-soluble member of B-complex vitamins, usually referred to as vitamin H; for more detailed stories about biotin, see Lane (2004). The structure of biotin was established by du Vigneaud (1942) in the beginning of the 1940s. Biotin acts as a CO₂ carrier, and in the pyruvate carboxylase reaction, it is linked to the epsilon-amino group of a lysine residue in the enzyme. Biotin is required for both metabolism and growth in humans, particularly regarding the niacin (vitamin B-3) metabolism and the production of fatty acids, antibodies as well as digestive enzymes.

In the early 1960s, Green synthesized [2'-¹⁴C] biotin using ¹⁴CO and measured the rate constants of avidin–biotin association (k_{on}) and dissociation (k_{off}) reactions. He obtained the first experimental results of k_{on} and k_{off} as $7 \times 10^7 \text{ M}^{-1}$ and $9 \times 10^{-8} \text{ s}^{-1}$, respectively. From these data, K_d (k_{off}/k_{on}) of the complex was estimated at about 10^{-15} M .

Into the three-dimensional space

The crystal structure of streptavidin bound with biotin was first determined in 1989 (Hendrickson *et al.*, 1989). The egg-white avidin in the deglycosylated form and complexed structure with biotin were determined in 1993 (Livnah *et al.*, 1993). Today, more than hundred structures of streptavidin and avidin are deposited in the Protein Data Bank (Berman *et al.*, 2000). Despite differences in the primary structure of the two proteins (~30% for sequence identity and 40% for similarity), both proteins have strikingly similar tertiary topology (β -barrels) and quaternary arrangements (homo-tetramer). In addition, both of them contain four biotin-binding sites wherein the interacting residues are also remarkably similar (Figure 1). Moreover, a critical tryptophan (Trp-110 in avidin and Trp-120 in streptavidin), provided by an adjacent monomer, plays a pivotal role in binding affinity with biotin and in stability of the tetrameric structure (Sano *et al.*, 1997; Freitag *et al.*, 1998; Laitinen *et al.*, 1999). Avidin and streptavidin in their apo forms show a disordered loop L3,4 (i.e. the loop connecting strands β 3 and β 4), an element related to exposure of the biotin-binding site to solvent. Upon the binding of biotin, the lid-like loop adopts an ordered and closed conformation to bury the biotin molecule inside the binding site (Hendrickson *et al.*, 1989; Weber *et al.*, 1989; Livnah *et al.*, 1993; Korndorfer and Skerra, 2002) and render the ligand almost inaccessible to solvent. The binding process involves a highly stabilized network of hydrogen bonds (Hyre *et al.*, 2006) and hydrophobic interactions. By counting the number of each interaction type, the presence of additional hydrophobic and hydrophilic groups in the binding site of avidin, while missing in streptavidin, may explain its higher affinity constant.

The avidin–biotin paradigm: or how to measure strong interactions?

The (strept)avidin–biotin complex allows the formation of multiple bonds due to its tetrameric structure, i.e. four binding sites for biotin. The binding avidity could self explain the high affinity observed between the two interacting molecules (Green, 1963a; Green, 1963b; Green, 1963c; Melamed and Green, 1963; Piran and Riordan, 1990). The complex is extremely stable over a wide range of temperature and pH but can be reversibly unbound in water at elevated temperature (Holmberg *et al.*, 2005).

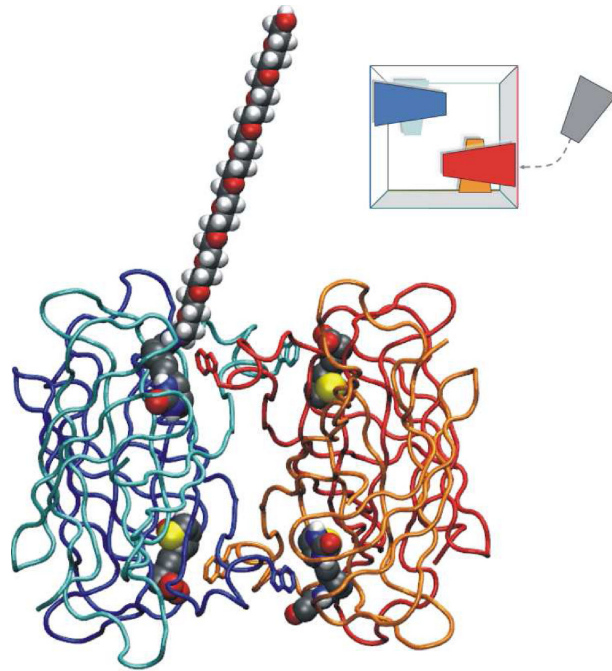


Figure 1. The tetrameric structure of streptavidin–biotin complex. The quaternary arrangements of the streptavidin tetramer were built based on the crystal structure (PDB code 2IZF, a dimeric form), drawn in blue and cyan (chains B and D, respectively). The other dimer (chains B' and D'), colored in red and orange, was constructed based on the symmetric rule defined in 2IZF. The biotin is drawn in colored CPK: gray for carbons, blue for nitrogens, red for oxygens, yellow for sulfurs, and white for hydrogens. The biotin from chain B is chemically linked to a 12-mer PEG linker. Each biotin binding pocket is closed by a Trp side chain (drawn in sticks) from another chain. Inset: schematic representation of the relative orientation of four biotin binding sites in streptavidin, a global view on accessibility of these binding sites. Figure drawn using VMD (Humphrey *et al.*, 1996).

In spite of some recent reports (Rao *et al.*, 1998; Chmura *et al.*, 2001; Butlin and Meares, 2006; Howarth *et al.*, 2006), (strept)avidin–biotin interaction is still considered as having the highest affinity via non-covalent bonding and whose unique properties can be used to offer universal technology and applications. Therefore, the avidin–biotin complex has been used as a model in numerous experimentations for characterization of binding affinity. This has been studied by a large variety of methods and different experimental setups (Figure 2 and Table I).

Direct characterization of biological reactions with a long lifetime (high affinity) is not easy in classical strategies. Most of the published results were obtained from estimation or by indirect methods such as competition assays. Recently, techniques have been developed to reduce the lifetime of intermolecular binding by an external force, including Biomembrane Force Probe (BFP), micropipettes, Flux chamber, and Atomic Force Microscopy (AFM).

However, characterization of the energy landscape of unbinding of (strept)avidin–biotin complex remains challenging. This system has been widely studied in many research groups and the results (Table II) are lacking for a consensus (Walton *et al.*, 2008). Hence, we attempt to re-characterize the energy landscape of this complex by explicitly taking into

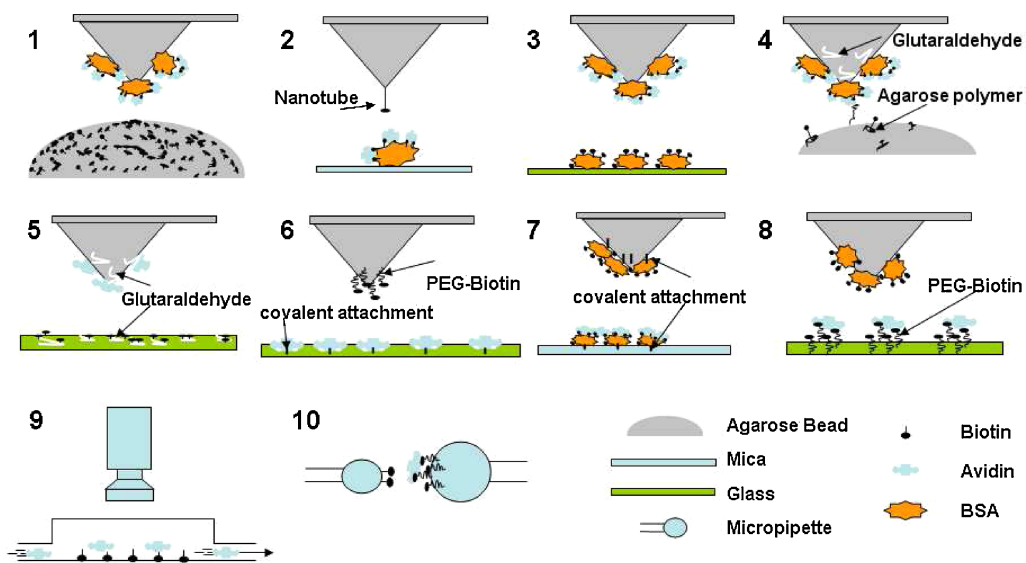


Figure 2. Summary of main constructions encountered in literature for measuring avidin–biotin interactions. AFM tips are represented by gray-colored triangles. Substrates made of mica or glasses are drawn as thin rectangles and that of agarose beads are presented as hemispheres. The cross-linkers, such as glutaraldehyde, are explicitly indicated. Sketch no. 9 describes laminar flow chamber equipments with a cyan-colored optical camera. Sketch no. 10 represents Biomembrane Force Probe (BFP) with biotin on the surface, and avidin is held by biotin which is covalently attached to the linkers on the micro-beads at the tip of the pipettes.

account the presence of multiple parallel interacting bonding resulting in multiple ruptures, which was not considered and addressed clearly in previous studies. Our results indicate that the apparent discrepancies found in the literature may be simply attributed to underestimating the influence of multiple parallel bonding.

MATERIAL AND METHODS

Preparations of gold-coated substrates

A flat gold-coated glass surface was prepared with 11-mercaptopoundecanoic acid (MUDA, Sigma-Adrich) in ethanol (1 mg/ml) for 30 min at room temperature. No particular attention was paid to making well-ordered self-assembled monolayers of MUDA. The substrate was rinsed with ethanol then with water. The substrate was incubated in 1 ml of V/V NHS/EDC (4 mg/ml ethyl-N-[3-diethylaminopropyl] carbodiimide (EDC, PIERCE) and 0.6 mg/ml N-hydroxysuccinimide (NHS, PIERCE) in water for 30 min. Then, 10 µg/ml streptavidin (Thermo scientific), avidin, or BSA (Sigma-Adrich) in acetate buffer (10 mM, pH 4) was deposited on the substrate surface for 60 min, followed by rinsing the substrate three times in phosphate buffer (10 mM, 50 mM NaCl, pH 7).

Functionalization of gold-coated tips

Gold-coated OBL (Olympus, short tip: $k = 0.03\text{--}0.009\text{ N/m}$, long tip: $k = 0.006\text{--}0.002\text{ N/m}$) or NPG (Veeco, $k = 0.32\text{--}0.06\text{ N/m}$) cantilevers were used. The tip was activated with 1 mM cysteamine (Sigma-Adrich) in ethanol during 30 min at room temperature. The cantilever was first rinsed once with ethanol and three times later with HEPES buffer (10 mM, 50 mM NaCl, pH 8). The coupling of biotin to the tip must be immediately performed using 50 mM of EZ-Link NHS-PEG12-Biotin (PIERCE)

stock solution in DMSO that was diluted up to 0.1 µM with the HEPES buffer for 60 min at room temperature. The cantilever was rinsed one time with 10 mM of HEPES buffer and then rinsed three times with phosphate buffer (10 mM, 50 mM NaCl, pH 7).

Experimental setups

A Dimension 3100 AFM microscope with a Nanoscope V controller (Digital Instrument Veeco, Santa Barbara, CA, USA) was used. The measurements of force–displacement curves were carried out using the pico-force mode in Nanoscope software (V7.30). In general, there are 5000 data points in each curve. We independently determined the spring constants of all individual gold-coated tips used (Olympus Biolever, Olympus—NPG Veeco) with the thermal tune module of the Nanoscope software. Calibration of a newly mounted tip was systematically performed. We obtained a wide range of loading rates, using linear speed with a closed-loop scanner by controlling either the reverse velocity of the piezo scanner or the spring constant of the cantilever. The scan rate in this study ranged from 60 nm/s to 3 µm/s.

Multiple parallel bonding and massive data analysis

Very few experiments have stressed on the study of multiple-bond ruptures (Hukkanen *et al.*, 2005; Levy and Maaloum, 2005; Sulchek *et al.*, 2005; Odorico *et al.*, 2007b; Teulon *et al.*, 2007; Tsukasaki *et al.*, 2007; Erdmann *et al.*, 2008; Guo *et al.*, 2008; Teulon *et al.*, 2008), a likely reason may be due to the difficulty in perceiving the distribution form of data that were collected and analyzed from the force–displacement (FD) curves obtained at different loading rates. The effective loading rate (r_e), is related to the critical force that ruptures the interaction between the functionalized tip and the molecules on the substrate surface (Odorico *et al.*, 2007b). Detected rupture events were sorted

Table I. Detail of the various experimental setups used to measure (strept)avidin-biotin interactions using AFM

Reference	Type	Tip		Object	Type	Linker	Substrate	Controls		Buffer	Scheme no. (Figure 2)
		κ (pN/nm)	Linker					pH	Conc		
(Florin et al., 1994)	Si ₃ N ₄	61 ± 10	BBSA ^a	Avidin	Agarose		Biotin	Saturation with biotin and avidin control BSA	7.4	140 mM NaCl	1
(Moy et al., 1994a)	Si ₃ N ₄	?	BBSA ^a	Avidin	Agarose		Biotin	Saturation with biotin and avidin control BSA	4–7–10	140 mM NaCl	1
(Wong et al., 1998)	Nanotube	500–5000		5-(biotin amido) pentylamine	Mica	Adsorption	Streptavidin	Unfunctionalized nanotube	7	PBS ^c	2
(Yuan et al., 2000)	Si ₃ N ₄	10–50	BBSA ^a	Streptavidin	Agarose		Biotin	Avidin free-biotin free	7.2	PBS	1
(Lo et al., 2001)	Si ₃ N ₄	39 ± 3	BBSA ^a	Streptavidin	Glass	BBSA ^a		Biotin–biotin bsa–bsa	7	PBS	3
(Wong et al., 1999)	Si ₃ N ₄	60	BBSA ^a	Avidin	Agarose	Agarose (100 nm)	Biotin	Saturation with biotin and avidin	7.2		4
(Lo et al., 1999)	Si ₃ N ₄	39, 150	BBSA ^a	(strept)avidin	Glass	BBSA		Stability of the measure Free avidin–streptavidin		PBS	3
(Zhang and Moy, 2003)	Si ₃ N ₄	~10	BBSA ^a	(strept)avidin	Agarose		Biotin		10–6		1
(de Odrowaz Piramowicz et al., 2006)	Si ₃ N ₄	10; 400	Glutaraldehyde	(strept)avidin	Glass	Glutaraldehyde	Biotin		7.2	150 mM NaCl	5
(Rico and Moy, 2007)	Si ₃ N ₄	10	BBSA ^a	Streptavidin	Agarose		Biotin			PBS	1
(Guo et al., 2008)	Si ₃ N ₄	155; 70; 260; 270	PEG ^b	Biotin	Glass	Ethanolamine	Streptavidin		7	PBS	6
(Walton et al., 2008)	Si ₃ N ₄	11; 35; 58; 121	BBSA ^a		Mica	BBSA ^a	Streptavidin			PBS	7
(Thormann et al., 2006)	Si ₃ N ₄	10–100	BBSA ^a		Glass	PEG ^b -biotin	Streptavidin			PBS	8
						BBSA ^a					3

^a Biotinylated bovine serum albumin (BBSA).^b Polyethylene glycol (PEG).^c PBS; 8 g/l NaCl; 0.2 g/l KCl; 1.44 g/l Na₂HPO₄; 0.24 g/l KH₂PO₄; pH 7.4.

Table II. Published data on (strept)avidin–biotin interactions studied by AFM or related techniques

Molecular partners Substrate-AFM tip	Scheme (Figure 2)	Average forces (pN)	Loading rate (pN/s)	γ (nm) ^a	k_{off} (s ⁻¹) ^b	ΔG^{\ddagger} (kJ mol ⁻¹) ^c	Ref.
Avidin–biotin	4	160 ± 20	0.9				(Florin et al., 1994)
Streptavidin/ Biotinylated BSA	3	125 ± 25					(Lee et al., 1994)
Avidin–biotin	1	175 pN					(Moy et al., 1994b)
Avidin–biotin (1)	8	160 ± 20					(Moy et al., 1994a)
Iminobiotin (2)		85 ± 10					
Streptavidin–biotin (3)		257 ± 25					
Avidin/desthiobiotin (4)		94 ± 10					
Streptavidin–biotin (5)		257 ± 25					
Streptavidin–Biotinylated BSA	3	253 ± 20					
Streptavidin–biotin	2	393 ± 10					
Streptavidin–biotinylated BSA	10	~200 (single) ↑ 5 pN to 170 pN					(Wong et al., 1998)
Avidin–biotin	10	Bond strength 0.05–10 000 10 000–60 000 0.05–30 30–10 000			0.5 0.12 3.0 0.3 to 0.5 0.12	6.14×10^{-5} 2.9	(Merkel et al., 1999)
Avidin–biotin	7	173 ± 19					(Merkel et al., 1999)
Biotin–streptavidin	1	326 ± 33					(Lo et al., 1999)
Streptavidin–biotin		126 ± 2.3					(Yuan et al., 2000)
Avidin–biotin		207 ± 5.8					
		2300					
		100–1000			0.49 (outer)	1.67×10^{-5}	
		1000–5000			0.05 (inner)	2.09	
		100–1000			0.53 (outer)	6.45×10^{-6}	
		1000–5000			0.2 (inner)	0.08	
		1600			2	10^{-3}	
Avidin–biotin	1				0.3	10	(DeParis et al., 2000)
Avidin–biotin	6/7	44 ± 3			0.56		
Streptavidin–Biotin	N/A ^d				0.48	85.69 ^f	(Galligan et al., 2001)
					0.23	77.33	
					0.12	36.37	
						7.11	
							(Continues)

Table II. (Continued)

Molecular partners Substrate-AFM tip	Scheme (Figure 2)	Average forces (pN)	Loading rate (pN/s)	γ (nm) ^a	k_{off} (s ⁻¹) ^b	ΔG^{\ddagger} (kJ mol ⁻¹) ^c	Ref.
Streptavidin–Biotinylated BSA	7	167 ± 20 236 ± 26 289 ± 13 350 ± 30 442 ± 17 150–500 pN 200	39–000 390–000 1950 000 3740 000 6 280 000 10^3 – 10^4 1267				(Lo <i>et al.</i> , 2001)
Streptavidin–biotin	4						(Zhang and Moy, 2003)
Streptavidin–biotin	5						(de Odrowaz Piramowicz <i>et al.</i> , 2006)
Avidin–biotin	5	236	300–1700 1700–9600 1382	0.081 ± 0.002 0.024 ± 0.003	0.56 ± 0.46 2.98 ± 2.61		(de Odrowaz Piramowicz <i>et al.</i> , 2006)
Streptavidin–biotin	N/A ^d	263 ± 36 378 ± 42 494 ± 39	300–1700 1700–9600 3900 39 000	0.073 ± 0.002 0.024 ± 0.002	0.25 ± 0.18 2.97 ± 2.71		(Zhou <i>et al.</i> , 2006)
Streptavidin–biotin	8		~200–113 000	0.64 0.072 (inner) 0.54	4×10^{-4} 13.46		(Thormann <i>et al.</i> , 2006)
Streptavidin–biotin	4	17°C 72 ± 2 95 ± 3 177 ± 4	338 ± 7 5977 ± 65 65 602 ± 758	17°C 0.35 ± 0.27 (outer) 17°C 0.09 ± 0.02 (inner) 24°C 0.38 ± 0.21 (outer)	0.02 ± 0.13 12 ± 9 0.10 ± 0.33		(Rico and Moy, 2007)
Streptavidin–biotin		37°C 27 ± 1 66 ± 2 121 ± 4	387 ± 9 6997 ± 94 69 457 ± 1055	24°C 0.09 ± 0.03 (inner) 37°C 0.31 ± 0.07 (outer) 37°C 0.15 ± 0.05 (inner)	23 ± 16 1.22 ± 0.93 15 ± 17		
Streptavidin–biotin	6			0.40 ± 0.05 0.44 ± 0.06 0.05 (MD) 0.11 (AFM)	0.23 0.27 5.1×10^{-9} to 2.1×10^{-7}	66.4 ± 1.6 ^g 66.0 ± 1.6	(Guo <i>et al.</i> , 2008) (Walton <i>et al.</i> , 2008)
Streptavidin–biotin	N/A ^d	46	301				This work
Avidin–biotin	6	75 (F^* 1) 135 (F^* 2) 195 (F^* 3) 260 (F^* 4)	1212	0.29 ± 0.05 (F^* 1 outer) 0.15 ± 0.02 (F^* 2 outer) 0.17 ± 0.05 (F^* 3 outer) 0.09 ± 0.01 (F^* 1 inner) 0.05 ± 0.003 (F^* 2 inner) 0.03 ± 0.003 (F^* 3 inner) 0.03 ± 0.002 (F^* 4 inner)	0.35 ± 0.35 ^e 0.38 ± 0.40 0.02 ± 0.04 13.07 ± 11.19 7.34 ± 3.99 4.43 ± 3.94 1.19 ± 0.86		

(Continues)

Table II. (Continued)

Molecular partners Substrate-AFM tip	Scheme (Figure 2)	Average forces (pN)	Loading rate (pN/s)	γ (nm) ^a	k_{off} (s^{-1}) ^b	ΔG^{\ddagger} (kJ mol $^{-1}$) ^c	Ref.
Streptavidin-biotin	6	68 (F*1) 120 (F*2) 260 (F*3)	1153 67–2208 67–2208 2208–162755 2208–162755 2208–162755	0.40 ± 0.08 (F*1 outer) 0.37 ± 0.14 (F*2 outer) 0.08 ± 0.004 (F*1 inner) 0.05 ± 0.002 (F*2 inner) 0.04 ± 0.004 (F*3 inner)	0.07 ± 0.09 0.002 ± 0.005 4.38 ± 2.47 4.09 ± 1.61 3.26 ± 3.54		This work

^a Energy barrier width in nm according to the Bell-Evans formalism.^b Kinetic dissociation rate constant in s^{-1} which is related to the energy barrier height.^c Kinetic activation energy in kJ/mol.^d Molecular dynamic simulations.^e $\sigma\gamma$ and σk_{off} are respectively the standard deviation of the Bell distance and of the constant of dissociation calculated according to Björnham and Schedin (2009).^f To calculate the activation energy from k_{on} the reciprocal of the attempt-to-escape frequency ($1/t_0$) was 10^9 s^{-1} .^g To calculate the activation energy from k_{on} the reciprocal of the attempt-to-escape frequency ($1/t_0$) was 10^{11} s^{-1} .

according to their r_e values, and the distribution from each consecutive interval of 100 r_e were fitted with multiple Gaussian functions.

Analysis of DFS measurements was done using the automatic software, YieldFinder. The treatments of FD records by YieldFinder are twofold: identify the rupture events and extract the force values responsible for the events (Odorico et al., 2007a). From the data processed by YieldFinder, we derived the force constant of the transducer system (made of MUDA, avidin, and PEG-biotin) based on the series-parallel spring model and the effective loading rates (Erdmann, 2005). This information can be further transformed into the energy landscape that characterizes the association/dissociation reaction of the molecular system.

Specific experimental controls

The most common negative controls in the study of the (strept)avidin-biotin system include: using non-functionalized tips or substrate surfaces, adding free ligands in the medium for blocking the interaction, and changing pH or salt concentrations in the medium. In this work, two negative controls were used (Figure 3); one is to saturate the (strept)avidin-coated surface with 10 μl of free Biotin solution (100 nM in phosphate buffer) to reach a final concentration of free Biotin around 5 nM; the other one consists in only coating BSA (Sigma-Aldrich) on the substrate at

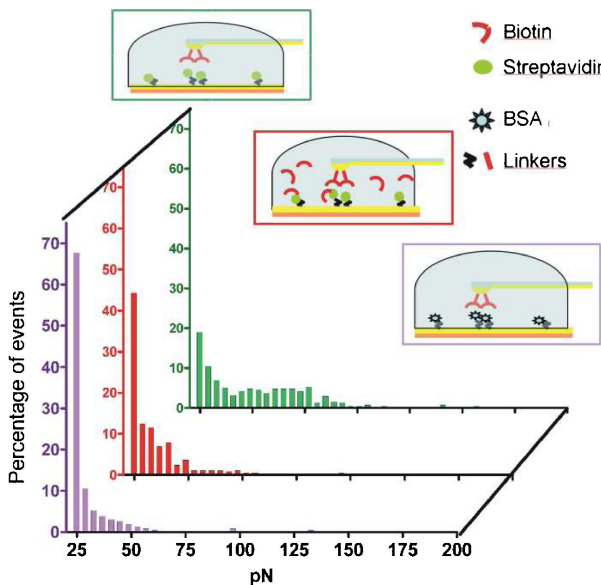


Figure 3. Three setups are presented to measure the rupture events of non-specific interactions. Each setup associated with its results was specified by a different color. The green box and the green histogram correspond to “positive” ruptures events: events attributed to specific interactions between biotin and streptavidin. In red, the design of experiment aims to inhibit the specific interaction between biotin and streptavidin by adding 0.1 μM of free biotin in the medium (in blue color) to saturate the binding sites of the receptor. The last negative control is presented in purple, where the streptavidin molecules were replaced by bovine serum albumin (blue star-shaped symbols). 1000–3000 experiments were performed for each setup. The calculated effective loading rates ranged from 3294 pN/s ($\ln(r_e) = 8.1$) down to 3 pN/s ($\ln(r_e) = 1.1$) for purple, to 4.5 pN/s ($\ln(r_e) = 1.5$) for green and to 9 pN/s ($\ln(r_e) = 2.2$) for red.

10 µg/ml in acetate buffer (10 mM, pH 4) for 60 min without any (strept)avidin.

RESULTS

According to the Bell-Evans model, the dissociation of two reactants catalyzed by an external force can be described by the transition state theory (Bell, 1978; Evans and Ritchie, 1997; Strunz *et al.*, 2000; Guthold *et al.*, 2001; Tinoco and Bustamante, 2002; Friedsam *et al.*, 2003). Provided with a linear force ramping, $F(t) = rt$, and a constant loading rate r , the most probable force to proceed the rupture event, i.e., the maximum of a probability distribution along the force ordinate axis, can be deduced from the classical kinetic theory as follows:

$$F^* = \frac{k_B T}{\gamma} \ln \frac{r_e \gamma}{k_{\text{off}} k_B T} \quad (1)$$

where k_B is the Boltzmann constant, T is the temperature, γ is the energy barrier width, k_0 is the off-rate, and r_e is the effective loading rate. One may obtain the value of γ by plotting F^* against $\ln(r_e)$ and k_0 from the slope of the fitting line.

The experimental setups of the present work can be described as sketch no. 6 shown in Figure 2. PEG-12 was chosen as the linker to attach biotin to the tip because it has a much shorter length than most of other linkers. Typical results of force-separation curves from the study system are shown in Figure 4A, where the retract trace of the cantilever away from the substrate is plotted from left to right. As previously reported (see references in Table I), the forces determined to rupture both avidin–biotin and streptavidin–biotin bonds depend on the loading rate of the applied force. Figure 4B shows the force histogram of rupture events, the black solid lines correspond to the Gaussian fitting results. The values of relevant parameters are co-listed in Table II with other published data. To provide a comparison with previous works, we selected rupture forces at a loading rate most often encountered in the Table II (around 1200 pN/s): F^{*1} is 75 pN for avidin–biotin binding and 68 pN for streptavidin–biotin complex. F^{*1} indicates the most probable rupture force for a single (strept)avidin–biotin bond. Similarly, F^{*2} and F^{*3} indicate the most probable rupture forces for double and triple bonds.

The Bell-Evans model revealed the presence of multiple segments (Figure 5A, B), which is a characteristic of multiple bond ruptures. The parameters, γ in nm and k_{off} in s⁻¹, that characterize the energy landscape are presented in Table II. As observed in most other experiments on (strept)avidin–biotin binding rupture, the presence of two loading rate regimes also appears from our results. At low loading rates (55–1808 pN/s or 4–7.5 in $\ln(r_e)$) four distinct segments for avidin–biotin and only three for streptavidin–biotin were observed. At high loading rates (1808–162755 pN/s or 7.5–12 in $\ln(r_e)$), five distinct segments were found for avidin–biotin but only four for streptavidin–biotin. Note that the first segments at both loading rates were attributed to non-specific interactions (purple lines in Figure 5). The need for multi-line fittings in each regime is attributed to the presence of multiple bonds involved in the interactions between (strept)avidin and biotin (Williams, 2003; Sulcik *et al.*, 2005; Odorico *et al.*, 2007b; Teulon *et al.*, 2007; Erdmann *et al.*, 2008). As described in the introduction, (strept)avidin can simultaneously form bonding with up to four biotins, the maximum number of multiple bonds observed

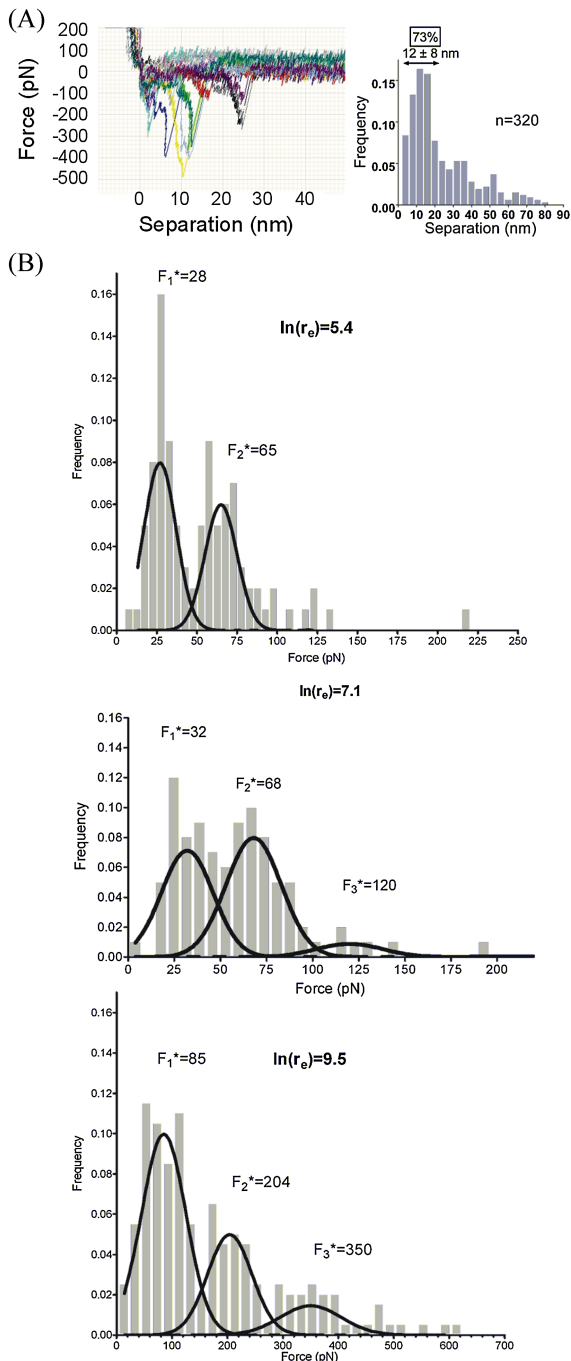


Figure 4. (A) Left, set of 15 force-separation curves that were extracted from experiments on the study of streptavidin–biotin interactions using Nanoscope software. On the right, most of rupture events occurred at a distance of 12 ± 8 nm representing 73% of rupture events in a set of 350 randomly chosen events. (B) Distribution of force histograms of rupture events for streptavidin–biotin binding. The results were obtained from the experimental setup no. 6 (Fig. 2) at loading rates 221 pN/s ($\ln(r_e) = 5.4$), 1212 pN/s ($\ln(r_e) = 7.1$), and 13360 pN/s ($\ln(r_e) = 9.5$), respectively. As indicated at the maximum of the Gaussian functions, the most probable forces (F^*) are determined.

from our experiments (Figure 5). However, depending on how (strept)avidin is oriented on the substrate plate, some biotin binding sites may be inaccessible to the biotinylated AFM tip.

DISCUSSION

Caution for analyzing force-displacement data

Force-displacement (FD) or force-distance measure represents the raw AFM experimental data for studying the binding-unbinding processes of an intermolecular system. During the approach procedure, or the so-called binding process, some care need to be taken for parameters such as contact time between the tip and the substrate, the force experienced at the contact point, and the density of receptors distributed over the substrate. For manifesting the specific interactions between a ligand and a receptor, one may choose an experimental condition in which enough contact time (but not too long), low force upon contact, and a flexible linker to attach the ligand and/or the receptor are demanded. On the other hand, how to detect and identify an unbinding event from a FD curve becomes a major issue in the procedure of tip retracting called as the unbinding

process. In particular, the identification of a rupture event corresponding to a specific interaction takes priority over searching for ruptures of single bond in FD measurements. Note that here single bond is specifically to indicate the interaction between one ligand and one receptor; one should not be confused with the definition in Chemistry such as covalent bonds, hydrogen bonds, or non-bonded interactions.

Several criteria to identify rupture events of single bond along with the rupture force were set as according to the following: (1) in the retract trace, no specific rupture event should be detected before the linker molecule pulled at the maximum length; (2) the last rupture event was considered as the preceding event to the cantilever released from the surface; (3) some small rupture peaks were discarded if their height is within the noisy range of the FD curve; (4) starting and ending points of an event peak should be located on the baseline. Needless to say, a widely accepted set of rules is important to achieve consensus on research results in the community. Unfortunately, only rare detail of systematic descriptions on this account is provided in literature. Another bottleneck in interpretations of DFS results on (strep)avidin–biotin interactions comes from the data fitting of force histograms. One may see later that statistically significant data points may play a critical role in accurately elucidating the energy landscape.

To obtain the values of most probable rupture force, Gaussian functions are in general introduced to fit the force histograms. However, the low number (~few hundreds) of collected measurements at a given loading rate may lead the fitting to a low degree of confidence. In addition, single-bond ruptures were usually the main pursuit. Accordingly, only a single Gaussian fit was applied in most of experiments and most efforts were made to follow this pursuit. However, a wide range of rupture force values can be found even for a single rupture peaks (Guo *et al.*, 2008). In another case where the delineation of multiple Gaussian fits was blurred at different loading rates, only the first population in different rate regimes was picked up for interpretations (Taranta *et al.*, 2008). This arbitrary choice may mislead our understanding of intermolecular interactions and, therefore, hamper reliability of DFS results.

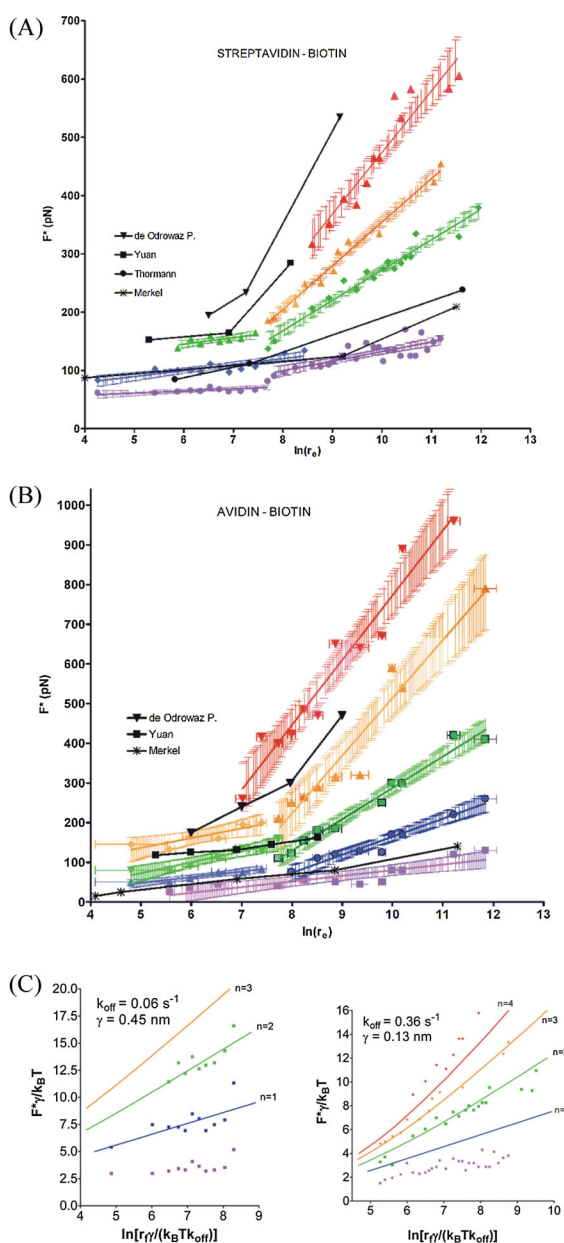


Figure 5. Plots of the most probable rupture forces F^* against the logarithm of effective loading rates $\ln(r_e)$. (A) Streptavidin–biotin interactions. (B) Avidin–Biotin interactions. The main plots for each system were made according to the Bell-Evans model. The most probable rupture forces are obtained within the 95% confidence intervals. Horizontal bars in (B) correspond to the dispersion of the loading rates from the distribution analysis. In both plots, two loading rate regimes are distinguishable. The outer energy barrier of dissociations for the two systems can be probed in the low loading rate regime whereas the inner barrier can be detected in the high loading rate regime. (C) Application of the Williams' formalism that characterizes the presence of multiple bonds by nonlinear fitting curves for the streptavidin–biotin complex at low loading rate (left) and high loading rate (right). The fitting lines are enumerated from the bottom to the top and kinetic parameters (k_{off} and γ) used to fit these lines are indicated on the top. It shows that the first lines in purple remained systematically unfit and therefore were attributed to non-specific rupture events. The remaining fits in blue, green, orange and red correspond to single, double, triple and quadruple parallel bonds. Black solid lines represent the fittings from the previously published results using the Bell-Evans model. ▼ (de Odrowaz Piramowicz *et al.*, 2006); ■ (Yuan *et al.*, 2000); ● (Thormann *et al.*, 2006); * (Merkel *et al.*, 1999).

Discrepancies in published results

As described above, the data treatments of FD measurements would be enough to derive an apparent discrepancy in characterization of (strept)avidin–biotin interactions (Table II). In order to tackle this problem, we have overlaid the previous results (Merkel *et al.*, 1999; Yuan *et al.*, 2000; de Odrowaz Piramowicz *et al.*, 2006; Thormann *et al.*, 2006) based on the Bell-Evans model with the present results and show them in Figure 5.

Most probable rupture forces obtained from Merkel *et al.* (1999) and Thormann *et al.* (2006) match those labeled single events in our study (Figure 5, blue curves) whereas those obtained from Yuan *et al.* (2000) match rupture forces attributed to double or triple events (Figure 5, green and orange curves). Finally, most probable rupture forces obtained by de Odrowaz Piramowicz *et al.* (2006) match those obtained for triple or quadruple events (Figure 5, orange and red curves). In fact, these results are easily explained by the experimental operating mode selected by these various authors (Table II). Indeed, experimental setups using (strept)avidin fixed on the substrate or on the pipette through PEG-biotins (Figure 2, no. 8 and no. 10) led to single rupture events likely because (strept)avidin was attached using at least triple biotin bonds leaving, therefore, only a single binding site for interaction. If it was not the case, singly or doubly biotin-bound (strept)avidin would have been displaced from the substrate ending up on the

moving tip. This present work emphasizes that these experiments targeted mostly single rupture events.

An intermediate situation was found for the experimental setup of Yuan *et al.* (2000) where the avidin was attached on the tip beforehand coated with biotinylated-BSA (Figure 2, no. 1). Knowing the structure of BSA, it is unlikely that more than two biotins would be available for attaching (strept)avidin. Consequently, this system is favorable to the probing of double or triple rupture events as evidenced from our analysis (Figure 5). Finally, experimental setups that chemically attach (strept)avidin on the substrate or the tip rather than using biotin (de Odrowaz Piramowicz *et al.*, 2006; and this work) allows the probing of all possible interactions ranging from single to quadruple events (Figure 5). Although we cannot exclude the hypothesis that the tip interacts with more than one deposited (strept)avidin, this is rather unlikely since no rupture events greater than 4 were consistently observed in our study. Consequently, the great variation observed in the analysis of the energy landscape of (strept)avidin–biotin is mostly due to operational aspects, a well-known trouble in affinity measurement (Azimzadeh *et al.*, 1992).

Naturally, the discrepancy in the results of Figure 5 will directly cause variations on the deduced values of energy landscape parameters: the energy barrier width ($0.1\text{--}30\text{ \AA}$) and the off-rate constant ($10^{-9}\text{--}13\text{ s}^{-1}$). One should be aware that a chemically linked biotin, e.g., with a PEG through an amide bond, exhibits different interactions from a free biotin (see Figure 6A and B).

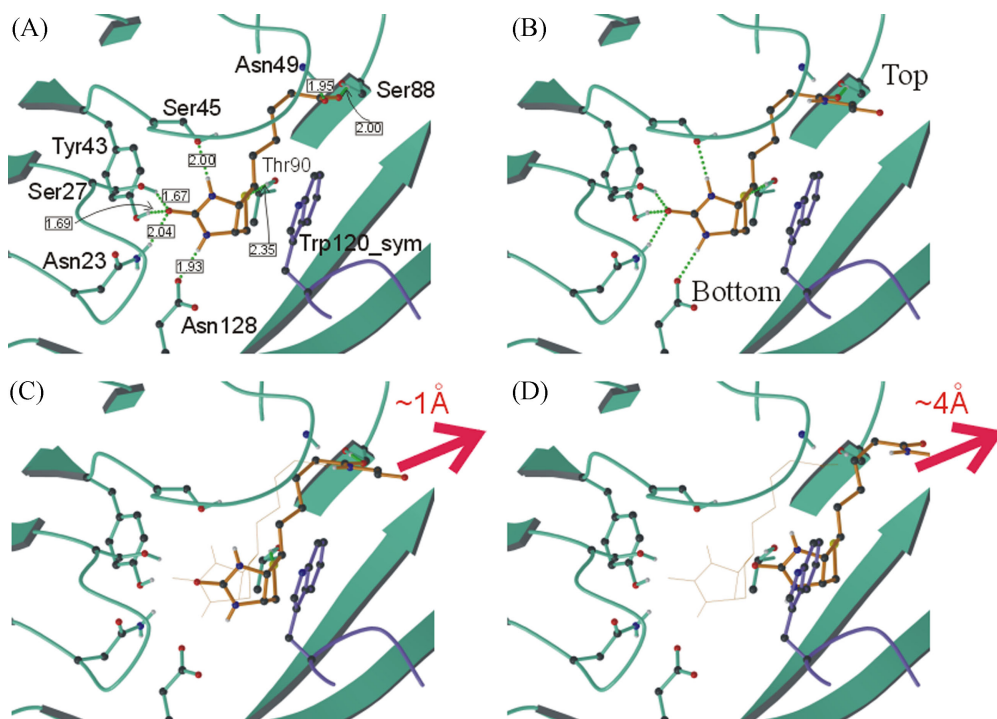


Figure 6. Structural analysis on streptavidin–biotin interactions. The PDB code for the crystal structure of streptavidin presented is 2IZF. Secondary structures are specified by arrows (β -strand); and turns/coils by tubes. Monomer D is drawn in cyan and Trp120 from the neighboring monomer is in purple. The ligand, biotin, is drawn as balls (colored atoms) and sticks (in orange). Side chains of monomer D are displayed by balls (colored atoms) and sticks (in cyan). (A) The structure of the biotin binding pocket in monomer D of streptavidin. The H-bond interactions are drawn in green dots. The number in the rectangles indicates the H-bond distance between streptavidin and biotin. The acceptable range of H-bond distance between the acceptor and hydrogen is within 2.5 \AA . (B) Same as A except that the formation of amide bond between biotin and the PEG linker (not shown) withdraws one native H-bond with streptavidin. For orientation purpose, the top and the bottom of the binding pocket is indicated. (C) Same as B but biotin was moved outwardly from the bottom of the binding pocket by about 1 \AA , leading to ruptures of all the H-bond interactions between biotin and the bottom of the binding pocket. However, biotin is still blocked by the side chain of Trp120 from a neighboring monomer. For comparison, the trace of the original position of biotin is illustrated in thin orange color. (D) Same as B but biotin was moved farther, about 4 \AA away from the bottom of the pocket. No H-bonding was found and biotin overcame the blockage of Trp120 from a neighboring monomer. Figure drawn using Molscript (Kraulis, 1991) and rendered using Raster3D (Merritt and Bacon, 1997).

Consequently, these factors may interfere with the estimated k_{off} , compared to that of free biotins in solution.

Energy landscape

According to the transition state theory, the attempt to escape from the bound state must overcome an energy barrier which is characterized by a width (γ) and a height ($\Delta G^\#$); as known, $\Delta G^\#$ is the activation energy and the kinetics dissociation rate $k_{\text{off}} = 1/\tau_0 \exp[-\Delta G^\#/k_B T]$, where τ_0 is the reciprocal of the attempt-to-escape frequency, k_B is the Boltzmann constant, and T is the temperature. The Bell-Evans model yields a linear relationship between the most probable rupture force and the logarithm of loading rate (see Equation (1)). However, most studies on (strept)avidin–biotin interactions have revealed a nonlinear tendency. Nonlinearity has been reasoned in literature as: (1) the presence of multiple energy barriers (Merkel *et al.*, 1999); (2) an asymmetric shape of the energy barrier, implying a relation such as $F^* \sim \ln(V)^{2/3}$ where V is the pulling velocity (Dudko *et al.*, 2003); (3) the effect of multiple parallel bonds (Williams, 2003); (4) artifacts from the data processing (Li *et al.*, 2010). One may not exclude the possibility that the nonlinearity can also come from a composite effect of the four factors mentioned above.

Two barriers were postulated in the energy landscape for unbinding the streptavidin–biotin complex (Merkel *et al.*, 1999) in agreement with kinetics of the exchange between unlabelled biotin and [^{14}C]biotin bound to avidin which revealed a biphasic dissociation phase (Green, 1963a). In contrast, some other authors insisted that the assumption of two energy barriers used in characterizing the energy landscape can be potentially misleading (Derenyi *et al.*, 2004; Neuert *et al.*, 2006). This reflects that the simplistic model of two energy barriers may be insufficient to interpret the underlying dissociation mechanism. Molecular dynamics and some hybrid simulations have also revealed several slips, suggesting a variety of unbinding pathways with multiple energy barriers (Izrailev *et al.*, 1997; Galligan *et al.*, 2001; Zhou *et al.*, 2006).

In this work, the nonlinear tendency was observed in our data analysis (see Figure 5). A clear cutoff occurs at 1808 and 2208 pN/s for avidin–biotin and for streptavidin–biotin unbinding, respectively. Within each regime of loading rate, no severe nonlinearity was observed on the Bell-Evans plot. Then we employed the Williams formalism (Williams, 2003) to extract information of multiple parallel bonds from each separate regime of loading rates. Thereby, a curvature found from data treatments of force normalization indicates the characteristic of multiple parallel bonds. The results for streptavidin–biotin are shown in Figure 5C. One advantage of applying Williams' formalism is to assign a multiplicity factor to each regression fit that highlights the non-specific interactions (the lowest fitting curves in the plots). Taking together with the Bell-Evans model and molecular structure analysis, we conclude that in the energy landscape two energy barriers are assumed in the unbinding process for the (strept)avidin–biotin complex.

The pathway of dissociation reactions

In the energy landscape of a dissociation reaction, if two energy barriers were found, the inner barrier is usually referred to a binding state close to the bound conformation, while the outer barrier marks the last state before the

unbound conformation. The function of an external force on intermolecular interactions is equivalent to a catalyst that reduces the activation energy associated with an energy barrier. Thereby, if the applied force along the reaction coordinate is high enough, some energy barriers may disappear as discussed previously (Evans and Ritchie, 1997; Merkel *et al.*, 1999). In short, at high loading rate the height of the outermost barrier is strongly reduced and, therefore, only the inner barrier is probed in the energy landscape.

Identification of unbinding processes has been performed using molecular dynamic simulations by counting, for instance, the hydrogen-bond (H-bond) ruptures (Zhou *et al.*, 2006); however, identification of transition barriers remains challenging. A consensus emerges on multiple studies of (strept)avidin–biotin interactions by DFS experiments: at least two energy barriers exist in the energy profile, one with a very narrow width ($\leq 1 \text{ \AA}$) and the other with a larger one ($\geq 4 \text{ \AA}$). The head chemical group of biotin contains limited degree of freedom while the carboxylic tail is extendable into the binding pocket (Figure 6A and B). Consequently, the narrow inner energy barrier is attributed to the event involved in breaking the H-bonds between biotin and streptavidin described as follows (Figure 6C). By moving only 1 \AA away from the bound conformation, the H-bond distance between the head chemical group of biotin and streptavidin is out of the range, $1.9 \pm 0.5 \text{ \AA}$, which defines the classical H-bond geometry, thus considered as ruptured. This does not imply that biotin totally escape from the binding pocket. On the structural view (Figure 6D), the steric effects exerted from Trp120 (Trp110 in avidin) on biotin during the unbinding process prevent biotin to escape. Consequently, the outer barrier characterized by a width of 4 \AA likely underlies the release mechanism of biotin passing over the Trp120 side chain. The visual inspection on the structure detects no further obstacle and biotin sets free from the gate of the binding pocket guarded by the Trp. This hypothesized mechanism can be tested by mutagenesis experiments. Mutating Trp120 to Phe has already been performed (Yuan *et al.*, 2000) and DFS results showed that the mutation not only reduced the outer energy barrier width but also increased the kinetic dissociation rate constant (lower affinity). The first observation is attributed to shrinking the Trp bulky side chain. The second one reflects that Phe raises the ease for biotin to run away from the binding pocket with smaller activation energy. In addition, the well-known loop L3,4 of (strept)avidin may contribute to the dynamic behavior of biotin through a H-bond network (Figure 6A) in the unbinding process (Merkel *et al.*, 1999; Yuan *et al.*, 2000) although the loop is expected to have a great impact on the association process.

CONCLUSION

In this paper, we provide an interpretation of discrepancies in previous studies, the so-called (strept)avidin–biotin paradox, by assuming the presence of multiple parallel bonds. Results for this system have been re-interpreted several times, including invoking the force history dependence for the largely scattering data obtained from different groups (Marshall *et al.*, 2005; Pincet and Husson, 2005), the experimental setups (Walton *et al.*, 2008) as well as data treatments (Guo, 2010). From the present DFS results, the dissociation of (strept)avidin–biotin complex undergoes two energy barriers which underlie two stages for the ligand to escape from the trap, i.e., the binding pocket. In addition, the

dissociation reaction involves breaking multiple parallel bonds, reflecting the structural character of (strept)avidin tetramer. It is noteworthy that molecular modeling is very helpful to elucidate the unbinding mechanism of ligand-receptor interactions by DFS experiments.

Acknowledgements

This work has been supported by the program for environmental nuclear toxicology of the Commissariat à l'énergie atomique et aux énergies alternatives (CEA), France.

REFERENCES

- Azimzadeh A, Pellequer JL, Van Regenmortel MHV. 1992. Operational aspects of antibody affinity constants measured by liquid-phase and solid-phase assays. *J. Mol. Recognit.* **5**: 9–18.
- Bell GI. 1978. Models for the specific adhesion of cells to cells. *Science* **200**: 618–627.
- Berman HM, Westbrook J, Feng Z, Gilliland G, Bhat TN, Weissig H, Shindyalov IN, Bourne PE. 2000. The protein data bank. *Nucleic Acids Res.* **28**: 235–242.
- Björnham O, Schedin S. 2009. Methods and estimations of uncertainties in single-molecule dynamic force spectroscopy. *Eur. Biophys. J.* **38**: 911–922.
- Butlin NG, Meares CF. 2006. Antibodies with infinite affinity: origins and applications. *Acc. Chem. Res.* **39**: 780–787.
- Chilkoti A, Boland T, Ratner BD, Stayton PS. 1995. The relationship between ligand-binding thermodynamics and protein-ligand interaction forces measured by atomic force microscopy. *Biophys. J.* **69**: 2125–2130.
- Chmura AJ, Orton MS, Meares CF. 2001. Antibodies with infinite affinity. *Proc. Natl. Acad. Sci. U.S.A.* **98**: 8480–8484.
- de Odrowaz Piramowicz M, Czuba P, Targosz M, Burda K, Szymonski M. 2006. Dynamic force measurements of avidin-biotin and streptavidin-biotin interactions using AFM. *Acta Biochim. Pol.* **53**: 93–100.
- DeParis R, Strunz T, Oroszlan K, Güntherodt H-J, Hegner M. 2000. Force spectroscopy and dynamics of the biotin-avidin bond studied by scanning force microscopy. *Single Mol.* **1**: 285–290.
- Derenyi I, Bartolo D, Ajdari A. 2004. Effects of intermediate bound states in dynamic force spectroscopy. *Biophys. J.* **86**: 1263–1269.
- du Vigneaud V. 1942. The structure of biotin. *Science* **96**: 455–461.
- Dudko OK, Filippov AE, Klafter J, Urbakh M. 2003. Beyond the conventional description of dynamic force spectroscopy of adhesion bonds. *Proc. Natl. Acad. Sci. U.S.A.* **100**: 11378–11381.
- Eakin RE, Snell EE, Williams RJ. 1940. A constituent of raw egg white capable of inactivating biotin *in vitro*. *J. Biol. Chem.* **136**: 801–802.
- Erdmann T. 2005. Stochastic Dynamics of Adhesion Clusters Under Force [doctor rerum naturalium]. Universitat Potsdam: Potsdam; 155.
- Erdmann T, Pierrat S, Nassoy P, Schwarz US. 2008. Dynamic force spectroscopy on multiple bonds: experiments and model. *Europhys. Lett.* **81**: 48001.
- Evans E, Ritchie K. 1997. Dynamic strength of molecular adhesion bonds. *Biophys. J.* **72**: 1541–1555.
- Florin EL, Moy VT, Gaub HE. 1994. Adhesion forces between individual ligand-receptor pairs. *Science* **264**: 415–417.
- Freitag S, Le Trong I, Chilkoti A, Klumb LA, Stayton PS, Stenkamp RE. 1998. Structural studies of binding site tryptophan mutants in the high-affinity streptavidin-biotin complex. *J. Mol. Biol.* **279**: 211–221.
- Friedsam C, Wehle AK, Kühner F, Gaub H. 2003. Dynamic single-molecule force spectroscopy: bond rupture analysis with variable spacer length. *J. Phys. Condens. Matter* **15**: 1709–1723.
- Galligan E, Roberts CJ, Davies MC, Tendler SJB, Williams PM. 2001. Simulating the dynamic strength of molecular interactions. *J. Chem. Phys.* **114**: 3208–3214.
- Green NM. 1963a. Avidin. 1. The use of (14-C)biotin for kinetic studies and for assay. *Biochem. J.* **89**: 585–591.
- Green NM. 1963b. Avidin. 3. The nature of the biotin-binding site. *Biochem. J.* **89**: 599–609.
- Green NM. 1963c. Avidin. 4. Stability at extremes of pH and dissociation into sub-units by guanidine hydrochloride. *Biochem. J.* **89**: 609–620.
- Green NM. 1975. Avidin. *Adv. Protein Chem.* **29**: 85–133.
- Guo S. 2010. Distributions of parameters and features of multiple bond ruptures in force spectroscopy by atomic force microscopy. *J. Phys. Chem. C* **114**: 8755–8765.
- Guo S, Ray C, Kirkpatrick A, Lad N, Akhremitchev B. 2008. Effects of multiple-bond ruptures on kinetic parameters extracted from force spectroscopy measurements: revisiting biotin-streptavidin interactions. *Biophys. J.* **95**: 3964–3976.
- Guthold M, Superfine R, Taylor RM. 2001. The rules are changing: force measurements on single molecule and how they relate to bulk reaction kinetics and energies. *Biomed. Microdevices* **3**: 9–18.
- Hendrickson WA, Pahler A, Smith JL, Satow Y, Merritt EA, Phizackerley RP. 1989. Crystal structure of core streptavidin determined from multi-wavelength anomalous diffraction of synchrotron radiation. *Proc. Natl. Acad. Sci. U.S.A.* **86**: 2190–2194.
- Holmberg A, Blomstergren A, Nord O, Lukacs M, Lundeberg J, Uhlen M. 2005. The biotin-streptavidin interaction can be reversibly broken using water at elevated temperatures. *Electrophoresis* **26**: 501–510.
- Howarth M, Chinnapan DJ, Gerrow K, Dorrestein PC, Grandy MR, Kelleher NL, El-Husseini A, Ting AY. 2006. A monovalent streptavidin with a single femtomolar biotin binding site. *Nat. Methods* **3**: 267–273.
- Hukkanen EL, Wieland JA, Gewirth A, Leckband DE, Braatz RD. 2005. Multiple-bond kinetics from single-molecule pulling experiments: evidence for multiple NCAM bonds. *Biophys. J.* **89**: 3434–3445.
- Humphrey W, Dalke A, Schulter K. 1996. VMD: visual molecular dynamics. *J. Mol. Graph.* **14**: 33–38.
- Hyre DE, Le Trong I, Merritt EA, Eccleston JF, Green NM, Stenkamp RE, Stayton PS. 2006. Cooperative hydrogen bond interactions in the streptavidin-biotin system. *Protein. Sci.* **15**: 459–467.
- Izrailev S, Stepaniants S, Balsera M, Oono Y, Schulter K. 1997. Molecular dynamics study of unbinding of the avidin-biotin complex. *Biophys. J.* **72**: 1568–1581.
- Koegl F, Toennis B. 1936. Über das bios-problem: Darstellung von krytallisiertem Biotin aus eigelb. *Z. Physiol. Chem.* **242**: 43–73.
- Korndorfer IP, Skerra A. 2002. Improved affinity of engineered streptavidin for the Strep-tag II peptide is due to a fixed open conformation of the lid-like loop at the binding site. *Protein Sci.* **11**: 883–893.
- Korpela J. 1984. Avidin, a high affinity biotin-binding protein, as a tool and subject of biological research. *Med. Biol.* **62**: 5–26.
- Kraulis PJ. 1991. MOLSCRIPT: a program to produce both detailed and schematic plots of protein structures. *J. Appl. Crystallogr.* **24**: 946–950.
- Kresge N. 2004. The discovery of avidin by Esmond E. Snell. *J. Biol. Chem.* **279**: e5.
- Laitinen OH, Airenne KJ, Marttila AT, Kulik T, Porkka E, Bayer EA, Wilchek M, Kulomaa MS. 1999. Mutation of a critical tryptophan to lysine in avidin or streptavidin may explain why sea urchin fibropellin adopts an avidin-like domain. *FEBS Lett.* **461**: 52–58.
- Lane MD. 2004. The biotin connection. *J. Biol. Chem.* 279.
- Lee GU, Kidwell DA, Colton RJ. 1994. Sensing discrete streptavidin-biotin interactions with atomic force microscopy. *Langmuir* **10**: 354–357.
- Levy R, Maaloum M. 2005. Specific molecular interactions by force spectroscopy: from single bonds to collective properties. *Biophys. Chem.* **117**: 233–237.
- Li N, Guo S, Akhremitchev BB. 2010. Apparent dependence of rupture force on loading rate in single-molecule force spectroscopy. *Chemphyschem* **11**: 2096–2098.
- Livnah O, Bayer EA, Wilchek M, Sussman JL. 1993. Three-dimensional structures of avidin and the avidin-biotin complex. *Proc. Natl. Acad. Sci. U.S.A.* **90**: 5076–5080.
- Lo Y-S, Huefner ND, Chan WS, Stevens F, Harris JM, Beebe TP. 1999. Specific interactions between biotin and avidin studied by atomic force microscopy using the Poisson statistical analysis method. *Langmuir* **15**: 1373–1382.

- Lo Y-S, Zhu Y-J, Beebe TP. 2001. Loading-rate dependence of individual ligand-receptor bond-rupture forces studied by atomic force microscopy. *Langmuir* **17**: 3741–3748.
- Marshall BT, Sarangapani KK, Lou J, McEver RP, Zhu C. 2005. Force history dependence of receptor-ligand dissociation. *Biophys. J.* **88**: 1458–1466.
- Melamed MD, Green NM. 1963. Avidin. 2. Purification and composition. *Biochem. J.* **89**: 591–599.
- Merkel R, Nassoy P, Leung A, Ritchie K, Evans E. 1999. Energy landscapes of receptor-ligand bonds explored with dynamic force spectroscopy. *Nature* **397**: 50–53.
- Merritt EA, Bacon DJ. 1997. Raster3D: photorealistic molecular graphics. *Meth. Enzymol.* **277**: 505–524.
- Moy VT, Florin EL, Gaub HE. 1994a. Intermolecular forces and energies between ligands and receptors. *Science* **266**: 257–259.
- Moy VT, Florin EL, Gaub HE. 1994b. Adhesive forces between ligand and receptor measured by AFM. *Colloids Surf. A* **93**: 343–348.
- Neuert G, Albrecht C, Pamir E, Gaub HE. 2006. Dynamic force spectroscopy of the digoxigenin-antibody complex. *FEBS Lett.* **580**: 505–509.
- Odorico M, Teulon J-M, Berthoumieu O, Chen SWW, Parot P, Pellequer J-L. 2007a. An integrated methodology for data processing in Dynamic Force Spectroscopy of ligand-receptor binding. *Ultramicroscopy* **107**: 887–894.
- Odorico M, Teulon J-M, Bellanger L, Vidaud C, Bessou T, Chen SWW, Quéméneur E, Parot P, Pellequer J-L. 2007b. Energy landscape of chelated uranyl—antibody interactions by Dynamic Force Spectroscopy. *Biophys. J.* **93**: 645–654.
- Pincet F, Husson J. 2005. The solution to the streptavidin-biotin paradox: the influence of history on the strength of single molecular bonds. *Biophys. J.* **89**: 4374–4381.
- Piran U, Riordan WJ. 1990. Dissociation rate constant of the biotin-streptavidin complex. *J. Immunol. Methods* **133**: 141–143.
- Rao J, Lahiri J, Isaacs L, Weis RM, Whitesides GM. 1998. A trivalent system from vancomycin-D-ala-D-Ala with higher affinity than avidin-biotin. *Science* **280**: 708–711.
- Rico F, Moy VT. 2007. Energy landscape roughness of the streptavidin-biotin interaction. *J. Mol. Recognit.* **20**: 495–501.
- Sano T, Vajda S, Smith CL, Cantor CR. 1997. Engineering subunit association of multisubunit proteins: a dimeric streptavidin. *Proc. Natl. Acad. Sci. U.S.A.* **94**: 6153–6158.
- Strunz T, Oroszlan K, Schumakovitch I, Guntherodt H, Hegner M. 2000. Model energy landscapes and the force-induced dissociation of ligand-receptor bonds. *Biophys. J.* **79**: 1206–1212.
- Sulcik TA, Friddle RW, Langry K, Lau EY, Albrecht H, Ratto TV, Denardo SJ, Colvin ME, Noy A. 2005. Dynamic force spectroscopy of parallel individual Mucin1-antibody bonds. *Proc. Natl. Acad. Sci. U.S.A.* **102**: 16638–16643.
- Taranta M, Bizzarri AR, Cannistraro S. 2008. Probing the interaction between p53 and the bacterial protein azurin by single molecule force spectroscopy. *J. Mol. Recognit.* **21**: 63–70.
- Teulon JM, Odorico M, Chen SWW, Parot P, Pellequer JL. 2007. On molecular recognition of an uranyl chelate by monoclonal antibodies. *J. Mol. Recognit.* **20**: 508–515.
- Teulon J-M, Parot P, Odorico M, Pellequer J-L. 2008. Deciphering the energy landscape of the interaction uranyl-DCP with antibodies using dynamic force spectroscopy. *Biophys. J.* **95**: L63–65.
- Thormann E, Hansen PL, Simonsen AC, Mouritsen OG. 2006. Dynamic force spectroscopy on soft molecular systems: improved analysis of unbinding spectra with varying linker compliance. *Colloids Surf. B Biointerfaces* **53**: 149–156.
- Tinoco I Jr, Bustamante C. 2002. The effect of force on thermodynamics and kinetics of single molecule reactions. *Biophys. Chem.* **101–102**: 513–533.
- Tsukasaki Y, Kitamura K, Shimizu K, Iwane AH, Takai Y, Yanagida T. 2007. Role of multiple bonds between the single cell adhesion molecules, nectin and cadherin, revealed by high sensitive force measurements. *J. Mol. Biol.* **367**: 996–1006.
- Walton EB, Lee S, Van Vliet KJ. 2008. Extending Bell's model: how force transducer stiffness alters measured unbinding forces and kinetics of molecular complexes. *Biophys. J.* **94**: 2621–2630.
- Weber PC, Ohlendorf DH, Wendoloski JJ, Salemme FR. 1989. Structural origins of high-affinity biotin binding to streptavidin. *Science* **243**: 85–88.
- Wilchek M, Bayer EA. 1990. Introduction to avidin-biotin technology. *Methods Enzymol.* **184**: 5–13.
- Williams PM. 2003. Analytical descriptions of dynamic force spectroscopy behaviour of multiple connections. *Anal. Chim. Acta* **479**: 107–115.
- Wong J, Chilkoti A, Moy VT. 1999. Direct force measurements of the streptavidin-biotin interaction. *Biomol. Eng.* **16**: 45–55.
- Wong SS, Joselevich E, Woolley AT, Cheung CL, Lieber CM. 1998. Covalently functionalized nanotubes as nanometer-sized probes in chemistry and biology. *Nature* **394**: 52–55.
- Yuan C, Chen A, Kolb P, Moy VT. 2000. Energy landscape of streptavidin-biotin complexes measured by atomic force microscopy. *Biochemistry* **39**: 10219–10223.
- Zhang X, Moy VT. 2003. Cooperative adhesion of ligand-receptor bonds. *Biophys. Chem.* **104**: 271–278.
- Zhou J, Zhang L, Leng Y, Tsao HK, Sheng YJ, Jiang S. 2006. Unbinding of the streptavidin-biotin complex by atomic force microscopy: a hybrid simulation study. *J. Chem. Phys.* **125**: 104905.